Molecular Biology of the Cell
Vol. 18, 4957–4968, December 2007

Synaptotagmin C2A Loop 2 Mediates Ca^{2+}-dependent SNARE Interactions Essential for Ca^{2+}-triggered Vesicle Exocytosis[D]

K. L. Lynch,*† R.R.L. Gerona,*† E. C. Larsen,*† R. F. Marcia,*‡ J. C. Mitchell,*‡ and T.F.J. Martin*

Departments of *Biochemistry and ‡Mathematics, University of Wisconsin, Madison, WI 53706

Submitted April 24, 2007; Revised September 21, 2007; Accepted September 26, 2007
Monitoring Editor: Patrick Brennwald

Synaptotagmins contain tandem C2 domains and function as Ca^{2+} sensors for vesicle exocytosis but the mechanism for coupling Ca^{2+} rises to membrane fusion remains undefined. Synaptotagmins bind SNAREs, essential components of the membrane fusion machinery, but the role of these interactions in Ca^{2+}-triggered vesicle exocytosis has not been directly assessed. We identified sites on synaptotagmin−1 that mediate Ca^{2+}-dependent SNAP25 binding by zero-length cross-linking. Mutation of these sites in C2A and C2B eliminated Ca^{2+}-dependent synaptotagmin−1 binding to SNAREs without affecting Ca^{2+}-dependent membrane binding. The mutants failed to confer Ca^{2+} regulation on SNARE-dependent liposome fusion and failed to restore Ca^{2+}-triggered vesicle exocytosis in synaptotagmin-deficient PC12 cells. The results provide direct evidence that Ca^{2+}-dependent SNARE binding by synaptotagmin is essential for Ca^{2+}-triggered vesicle exocytosis and that Ca^{2+}-dependent membrane binding by itself is insufficient to trigger fusion. A structure-based model of the SNARE-binding surface of C2A provided a new view of how Ca^{2+}-dependent SNARE and membrane binding occur simultaneously.

INTRODUCTION

Neurotransmitter, neuropeptide, and peptide hormone secretion is mediated by the fusion of vesicles with the plasma membrane in a reaction catalyzed by soluble *N*-ethylmaleimide–sensitive factor attachment protein receptor (SNARE) complexes. The vesicle SNARE VAMP-2 (aka synaptobrevin) assembles into a four-helix bundle with the plasma membrane SNAREs, SNAP25 and syntaxin-1 (Sollner *et al.*, 1993a; Hayashi *et al.*, 1994; Fasshauer *et al.*, 1997; Poirier *et al.*, 1998; Sutton *et al.*, 1998), to promote close phospholipid bilayer apposition and potentially drive membrane fusion (Weber *et al.*, 1998).

Peptide and transmitter release by SNARE complex–dependent vesicle exocytosis is tightly regulated by cytoplasmic Ca^{2+} (Douglas and Rubin, 1961; Katz and Miledi, 1965). Synaptotagmin proteins possess the requisite Ca^{2+}-binding properties to serve as Ca^{2+} sensors that regulate vesicle exocytosis (Brose *et al.*, 1992; Chapman, 2002; Sudhof, 2002; Rizo *et al.*, 2006). Consistent with a Ca^{2+}-sensor role, synaptotagmin−1 is essential for fast synchronous Ca^{2+}-triggered neurotransmitter release (Geppert *et al.*, 1994; Littleton *et al.*, 1994) and mutant alleles alter the Ca^{2+}-dependence of neurotransmitter release (Fernandez-Chacon *et al.*, 2001; Littleton *et al.*, 2001; Rhee *et al.*, 2005). Ca^{2+} regulation of vesicle fusion is fully abrogated in cells that lack vesicle-resident synaptotagmins (Lynch and Martin, 2007). The cytoplasmic domain of synaptotagmin−1 (C2AB) also confers Ca^{2+} stimulation on SNARE-dependent liposome fusion in vitro (Tucker *et al.*, 2004). The precise mechanism by which synaptotagmins mediate the coupling of cytoplasmic Ca^{2+} rises in vivo to SNARE-dependent vesicle fusion is incompletely understood.

Synaptotagmin−1 is composed of N-terminal luminal and transmembrane domains and a cytoplasmic domain containing membrane-proximal (C2A) and membrane-distal (C2B) C2 domains connected by a short linker. Five aspartates plus other residues in loops 1 and 3 of the eight-stranded β-sandwich C2 domains ligate 3 and 2 Ca^{2+} ions in C2A and C2B, respectively (Sutton *et al.*, 1995, 1999; Ubach *et al.*, 1998; Fernandez-Chacon *et al.*, 2001). The intrinsic affinity for Ca^{2+} is quite low (Fernandez-Chacon *et al.*, 2002) but is markedly enhanced by the interaction of the C2 domains with bilayers containing acidic phospholipids such as phosphatidylserine (PS; Zhang *et al.*, 1998). Interactions with PS complete the Ca^{2+}-binding sites on loops 1 and 3, and adjacent hydrophobic residues at the tips of these loops insert into the bilayer (Zhang *et al.*, 1998; Bai *et al.*, 2002; Frazier *et al.*, 2003). Ca^{2+}-dependent synaptotagmin binding to PS is an important coupling element in Ca^{2+}-triggered vesicle fusion. Mutation of C2A loop 3 R233 reduces the Ca^{2+} affinity for PS binding by synaptotagmin−1 and reduces the Ca^{2+}-depen-

This article was published online ahead of print in *MBC in Press* (http://www.molbiolcell.org/cgi/doi/10.1091/mbc.E07–04–0368) on October 3, 2007.

[D] The online version of this article contains supplemental material at *MBC Online* (http://www.molbiolcell.org).

† These authors contributed equally to this work.

Address correspondence to: T.F.J. Martin (tfmartin@wisc.edu).

Abbreviations used: SNAREs, soluble *N*-ethylmaleimide-sensitive factor attachment protein receptors; SNAP25, synaptosomal associated protein of 25 kDa; VAMP, vesicle-associated membrane protein; PS, phosphatidylserine; PIP2, phosphatidylinositol-4,5-bisphosphate; TIRF, total internal reflection fluorescence; ANF-EGFP, atrial naturetic factor-enhanced green fluorescent protein; CgB, chromogranin B.

dent probability of transmitter release (Fernandez-Chacon *et al.*, 2001). Conversely, mutation of hydrophobic residues in the Ca^{2+}-binding loops 1 and 3 to tryptophan enhances the Ca^{2+} affinity for PS binding and correspondingly increases the Ca^{2+}-dependent probability of transmitter release (Rhee *et al.*, 2005). The ability of synaptotagmin C2AB to confer Ca^{2+} stimulation on SNARE-dependent liposome fusion also depends upon the presence of PS in liposomes (Bhalla *et al.*, 2005). These findings indicate that PS-binding by synaptotagmin−1 is essential for coupling Ca^{2+} increases to membrane fusion.

Synaptotagmins also exhibit Ca^{2+}-independent and -dependent interactions with SNARE proteins in vitro. Synaptotagmin−1 is coisolated with SNARE complexes from brain detergent extracts in the absence of Ca^{2+} (Bennett *et al.*, 1992; Sollner *et al.*, 1993a; Schiavo *et al.*, 1997). However, synaptotagmin−1 also engages in Ca^{2+}-stimulated interactions with syntaxin-1 and SNAP25 (Chapman *et al.*, 1995; Li *et al.*, 1995; Kee and Scheller, 1996; Davis *et al.*, 1999; Gerona *et al.*, 2000) as well as with heterodimeric and heterotrimeric SNARE complexes (Davis *et al.*, 1999; Gerona *et al.*, 2000). Ca^{2+}-dependent synaptotagmin-SNARE interactions provide an appealing mechanism for coupling Ca^{2+} rises to membrane fusion but the physiological role of this interaction has not been directly assessed. A major reason for this is the lack of information on regions in synaptotagmin that mediate SNARE interactions. Although NMR and crystal structures for synaptotagmin and SNARE complexes have been solved (Sutton *et al.*, 1995, 1998, 1999; Shao *et al.*, 1998; Fernandez-Chacon *et al.*, 2001; Fernandez *et al.*, 2001; Ernst and Brunger, 2003), structures of synaptotagmin-bound SNARE complexes are not yet available. Thus, precise point mutations in synaptotagmin that selectively affect SNARE binding without affecting PS binding have not been available to critically assess the functional role of Ca^{2+}-dependent synaptotagmin-SNARE interactions.

In the current work, we identified sites on synaptotagmin−1 that bind SNAP25 using zero-length cross-linking. Mutation of sites in C2A and C2B was found to eliminate Ca^{2+}-dependent synaptotagmin−1 binding to SNARE complexes without affecting PS- or phosphatidylinositol-4,5-bisphosphate (PIP_2)-containing membrane binding. The mutations eliminated the Ca^{2+} stimulation of SNARE-dependent liposome fusion by synaptotagmin−1 and prevented the restoration by synaptotagmin−1 of Ca^{2+}-triggered vesicle exocytosis in synaptotagmin-deficient PC12 cells. A structure-based model of C2A loop 2 interactions with the C-terminus of SNAP25 provided a novel view of simultaneous Ca^{2+}-dependent SNARE and membrane binding that accounts for previous findings on synaptotagmin−1 function.

MATERIALS AND METHODS

Antibodies and DNA Constructs

Antibodies used were synaptotagmin−1 monoclonal (clone 604.1; Synaptic Systems, Göttingen, Germany); SNAP25 monoclonal (Sternberger Monoclonals, Baltimore, MD); and CgB monoclonal (generously provided by W. Huttner, Max Plânck Institute of Molecular Cell Biology and Genetics, Dresden, Germany). A synaptotagmin−1 polyclonal antibody was generated using a synaptotagmin−1 C2AB fusion protein. Plasmid pGEX-2T (Amersham Pharmacia Biotech, Piscataway, NJ) was used for *Escherichia coli* expression of recombinant proteins. The vectors encoding synaptotagmin−1 C2AB, C2A, and C2B, SNAP25B, and VAMP2 were kindly provided by R. H. Scheller (Genentech). Vectors encoding syntaxin 1A and synaptotagmin−1 were kindly provided by E. Chapman (University of Wisconsin). Glutathione *S*-transferase (GST) fusion proteins were produced in *E. coli* by standard methods and purified by glutathione-agarose chromatography (Amersham Pharmacia Biotech). Synaptotagmin−1 C2AB was purified on glutathione-Sepharose 4B using nuclease and high-salt washes to remove contaminants (Tucker *et al.*, 2003). Plasmids for generating full-length syntaxin and SNAP25 heterodimer (pTW34) and full-length VAMP2 (pTW2) were generously provided by J. E. Rothman (Columbia University) and T. Weber (Columbia University). The plasmid encoding ANF-EGFP was kindly provided by E. Levitan (University of Pittsburgh School of Medicine, Pittsburgh, PA). Oligonucleotides encoding synaptotagmin−1/-9 short hairpin RNAs (shRNAs; Lynch and Martin, 2007) were ligated into pSHAG-1 vector (Paddison *et al.*, 2002) via BamHI and BseRI sites. The open reading frame of synaptotagmin−1 was reverse-transcribed and PCR-amplified from rat PC12 cells and ligated into pcDNA3.1 (Invitrogen, Carlsbad, CA). The QuickChange Site-Directed Mutagenesis method (Stratagene, La Jolla, CA) was used to generate the synaptotagmin−1 silent mutant, pcDNA3-syt I sm (Lynch and Martin, 2007) and synaptotagmin−1 mutants in pGEX-2T-syt I C2AB and pcDNA3-syt I sm.

Cross-Linking and Mass Spectrometric Analysis

The SNAP25 protein used in binding and cross-linking studies exhibited 68% α-helical content (estimated by circular dichroism), indicating that it was natively folded. Previous studies (Gerona *et al.*, 2000) indicated that synaptotagmin bound SNAP25 and SNAP25/syntaxin heterodimers similarly. Cross-linking was performed in 1-ml reactions containing 20 mM HEPES (pH 7.2), 150 mM KCl, and 2 mM EGTA or 1 mM $CaCl_2$. Wild-type C2AB, 1 μM, or oligomerization-deficient (Chapman *et al.*, 1998) C2AB K326A/K327A and 1 μM SNAP25 were incubated for 2 h at 4°C, followed by an additional 2-h incubation at 4°C in the presence of 2 mM 1-ethyl-3-[3-dimethylaminopropyl] carbodiimide hydrochloride (EDC) and 5 mM *N*-hydroxysulfosuccinimide (sulfo-NHS; Pierce Chemical, Rockford, IL). Cross-linking was quenched by the addition of 10 mM hydroxylamine. Protein was precipitated in 10% trichloroacetic acid and analyzed by SDS-PAGE for staining with colloidal Coomassie Blue. Protein bands were excised, washed and destained and gel fragments were reduced, alkylated, and digested with trypsin. Peptides were extracted and subjected to MALDI mass spectrometry at the University of Wisconsin-Madison Biotechnology Mass Spectrometry Facility. Peptide identity was determined using the MS Digest program (UCSF Protein Prospector). Results in Figure 1 are representative of three experiments, with similar results for C2AB or oligomerization-deficient C2AB K326A/K327A.

SNARE-containing Liposomes, Fusion Assay, and Binding Studies

All lipids were purchased from Avanti Polar Lipids (Alabaster, AL). Incorporation of VAMP-2 and SNAP25/syntaxin-1 into liposomes was conducted as described (Weber *et al.*, 1998). VAMP-2 liposomes were formed by dialysis using a lipid mix comprised of 82% 1,2-dioleoyl-sn-glycero-phosphatidylcholine (DOPC), 15% 1,2-dioleoyl-sn-glycero-phosphatidylserine (DOPS), 1.5% *N*-(7-nitro-2–1,3-benzoxadizol-4-yl)-1,2-dipalmitoyl-sn-glycero-phosphatidylethanolamine (NBD-PE, donor), and 1.5% *N*-(lissamine rhodamine B sulfonyl)-1,2-dipalmitoyl-sn-glycero-phosphatidylethanolamine (Rh-PE, acceptor). SNAP25/syntaxin-1 liposomes were formed from 85% DOPS and 15% DOPC (mol/mol). VAMP-2 and SNAP25/syntaxin-1 liposomes contained ~90 copies or ~80 copies of proteins/liposome, respectively. Fusion assays were carried out as described (Weber *et al.*, 1998; Tucker *et al.*, 2004). t-SNARE liposomes, 45 μl, and 5 μl of NBD/Rhodamine-PE–labeled v-SNARE liposomes along with 10 μM C2AB or mutants in reconstitution buffer (10 mM HEPES, 150 mM KCl) were mixed in either 0.2 mM EGTA or the indicated concentration of Ca^{2+} in a total volume of 75 μl. NBD fluorescence was monitored for 2 h at 37°C. Dodecylmaltoside was added to a final concentration of 1% vol/vol, and NBD fluorescence was monitored for an additional 10 min. Data were plotted as % maximum NBD fluorescence and curve fitting was carried out using Prism 3.0 software with the variable slope sigmoidal dose–response function.

Flotation assays were carried out as described (Tucker *et al.*, 2004) with modifications. Liposomes containing SNAP25 and syntaxin were mixed with 10 μM C2AB in either 0.2 mM EGTA or the indicated concentration of Ca^{2+} and subject to buoyant density flotation on Accudenz gradients (40, 30, and 0% vol/vol) by centrifugation at 45,000 rpm at 4°C for 4 h. Material at the 0%/30% interface was collected, analyzed by SDS gel electrophoresis and stained with colloidal Coomassie Blue. Coomassie-stained bands were quantified with a Molecular Dynamics SI Densitometer using Image Quant software (Sunnyvale, CA).

Binding studies for Figure 3a were conducted in 200 μl reactions containing 20 mM HEPES (pH 7.2), 150 mM KCl, 2 mM EGTA or 1 mM $CaCl_2$, 1% Triton X-100, and 0.5% cold fish skin gelatin (Sigma, St. Louis, MO). Ternary SNARE complexes were formed by overnight incubation at 4°C of equimolar amounts of SNAP25, VAMP, and GST-syntaxin. Glutathione-agarose beads containing 1 μM GST-SNARE complex were incubated with 1 μM C2AB. After a 2-h incubation at 4°C, beads were recovered by centrifugation, washed, eluted in sample buffer, and analyzed by SDS-PAGE and immunoblotting with synaptotagmin antibody using enhanced chemiluminescence with horseradish peroxidase–conjugated goat anti-rabbit IgG (Pierce Chemical). Western blots were quantified with a Molecular Dynamics SI Densitometer using Image Quant software.

Cell Culture, Transfection, Immunoblot Analysis, and Immunocytochemistry

PC12 cells were cultured in DMEM supplemented with 5% horse serum and 5% calf serum. Transfection was conducted by electroporation using an Electroporator II (Invitrogen). The synaptotagmin−1/9-null PC12 cell line was isolated as described previously (Lynch and Martin, 2007). Protein expression levels were determined from total cell lysates prepared in 1 mM phenylmethylsulfonyl fluoride and 1% Triton X-100 and clarified by centrifugation at 16000 × *g* for 5 min. Total protein, 20 μg, determined by bicinchoninic acid (BCA; Pierce Chemical) was loaded per lane for gel electrophoresis. Immunoblot analysis was conducted by standard methods.

For immunocytochemistry, cells were plated on poly-DL-lysine– and collagen-coated coverslips. Cells were washed with phosphate-buffered saline (PBS), fixed with 4% formaldehyde (wt/vol), permeabilized with 0.3% Triton X-100 in PBS, and blocked in 10% fetal bovine serum (FBS) in PBS. Primary and secondary antibodies were diluted in FBS blocking solution. Coverslips were mounted on slides with Mowiol 4–88 Reagent (Calbiochem, La Jolla, CA), and cells were imaged on a Nikon C1 laser scanning confocal microscope (Melville, NY) with a 60× oil immersion objective with NA 1.4. Z-series images were obtained with 250-nm sectioning with oversampling. The resulting Z-stacks were deconvolved using Autodeblur/autovisualize software (AutoQuant Imaging, Rochester, NY).

Exocytosis Assay

Cells were transiently transfected and plated on 35-mm glass-bottom dishes (MatTek, Ashland, MA) coated with poly-DL-lysine and collagen. After 48 h, cells were imaged on a Nikon total internal reflection fluorescence (TIRF) Microscope Evanescent Wave Imaging System on a TE2000-U Inverted Microscope (Nikon) and an Apo TIRF 100×, NA 1.45 (Nikon) objective lens. Enhanced green fluorescent protein (EGFP) fluorescence was excited with the 488-nm laser line of an argon ion laser. Cells were imaged in basal media (15 mM HEPES, pH 7.4, 145 mM NaCl, 5.6 mM KCl, 2.2 mM $CaCl_2$, 0.5 mM $MgCl_2$, 5.6 mM glucose, 0.5 mM ascorbic acid, and 0.1% bovine serum albumin [BSA]) or depolarization medium (same as basal medium with 95 mM NaCl and 56 mM KCl). Images were acquired at 250-ms intervals with a CoolSNAP-ES Digital Monochrome CCD camera system (Photometrics, Woburn, MA) controlled by Metamorph software (Universal Imaging, West Chester, PA). All analysis was done using Metamorph software (Universal Imaging).

RESULTS

Ca^{2+} Stimulates the Formation of a Synaptotagmin-SNAP25 Cross-linked Product

Acidic residues in the C-terminus of SNAP25 are required for Ca^{2+}-dependent synaptotagmin−1 binding and Ca^{2+}-triggered vesicle exocytosis (Zhang *et al.*, 2002). To determine the sites on both proteins that mediate synaptotagmin−1 interactions with SNAP25, we used cross-linking with EDC and sulfo-NHS. Synaptotagmin binding to SNARE proteins is electrostatic (Tang *et al.*, 2006) and the zero-length cross-linker EDC converts carboxylate and amine groups in close proximity to amide bonds.

A cross-linked adduct containing the cytoplasmic domain of synaptotagmin−1 (termed C2AB) and SNAP25 was observed in both the absence and presence of Ca^{2+} (Figure 1a). The molecular weight of the C2AB-SNAP25 adduct (~65 kDa) indicated that it consisted of one C2AB cross-linked to one SNAP25, as anticipated from the stoichiometry of binding (Davis *et al.*, 1999; Gerona *et al.*, 2000). The presence of Ca^{2+} markedly enhanced the yield of cross-linked C2AB-SNAP25 (Figure 1a) similar to the effect of Ca^{2+} in binding studies (Davis *et al.*, 1999; Gerona *et al.*, 2000). At the protein concentrations used (1 μM), we detected very little cross-linking of either C2A or C2B with SNAP25 in the absence or presence of Ca^{2+} (Figure 1b), which is similar to previous binding studies (Schiavo *et al.*, 1997; Gerona *et al.*, 2000; Tucker *et al.*, 2003). These studies confirmed that both C2 domains in C2AB are required for optimal binding to SNAP25 and that this interaction is strongly stimulated by Ca^{2+}.

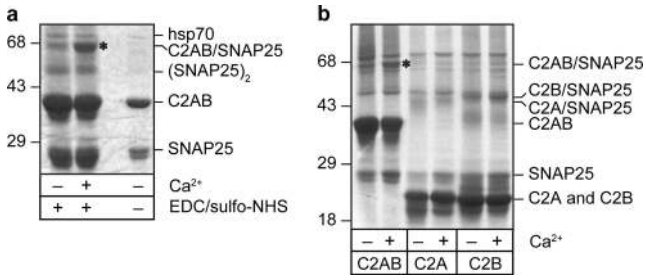

Figure 1. Ca^{2+} stimulates the formation of a C2AB-SNAP25 cross-linked adduct. (a) Wild-type C2AB (not shown) or C2AB K326A/K327A (1 μM) and SNAP25 (1 μM) were incubated in the absence (−) or presence (+) of 1 mM $CaCl_2$ before the addition of cross-linker (EDC/sulfo-NHS) and analyzed by SDS PAGE with Coomassie staining. C2AB K326A/K327A was used to minimize oligomerization (Chapman *et al.*, 1998), but identical results were obtained with wild-type C2AB and no self cross-linking of C2AB was observed. Bands corresponding to SNAP25, C2AB, SNAP25 dimer, C2AB-SNAP25 adduct (*), and hsp70 are indicated. Lane on right was loaded with 10% input lacking cross-linker. (b) Both C2 domains are required for optimal cross-linking of C2AB to SNAP25. C2AB, C2A, or C2B fusion proteins (1 μM) were incubated with SNAP25 (1 μM) in the absence (−) or presence (+) of 1 mM Ca^{2+} before cross-linking. Bands corresponding to C2AB-SNAP25 (*), C2B-SNAP25, C2A-SNAP25, or free proteins are indicated.

Mass Spectrometric Analysis of the Synaptotagmin-SNAP25 Cross-Links

To identify points of interaction between C2AB and SNAP25, we determined the sites of cross-linking by trypsin digestion and mass spectrometric analysis of proteolytic fragments. Parallel samples of C2AB or SNAP25 alone or the C2AB-SNAP25 adduct were digested with trypsin and analyzed by mass spectrometry. Our sequence coverage by MALDI was ~73% for C2AB and ~83% for SNAP25. To detect sites where cross-linking occurred, we identified mass/charge peaks present in C2AB and SNAP25 digests that were absent in the digest of cross-linked C2AB-SNAP25, which correspond to peptides in either protein that were cross-linked. We then identified mass/charge peaks that were unique to the cross-linked C2AB-SNAP25 adduct but were absent in C2AB and SNAP25 samples. These peaks correspond to cross-linked peptides. The assignment results are summarized in Table 1 and schematically depicted in Figure 2.

This analysis identified three interfaces for C2AB and SNAP25 interactions based on the assignments of peaks unique to the cross-linked adduct. One interaction was entirely Ca^{2+}-dependent, another was observed only in the absence of Ca^{2+}, and the third was observed in both the presence and absence of Ca^{2+} (Table 1; +, −, and ± Ca^{2+}, respectively). The first of these interactions, indicated by unique peaks with mass/charge ratios of 1669.6, 1685.9, 1696.8, and 1160.7, were detected only in the presence of Ca^{2+}. These peaks correspond to regions of SNAP25 (176-201) cross-linked to regions of synaptotagmin (191-200; Table 1). This indicated that residues of the basic β4-loop 2 region of synaptotagmin−1 C2A bind to C-terminal helix acidic residues in SNAP25 (Figure 2). The results strongly confirmed our previous finding that C-terminal SNAP25 acidic residues are essential for Ca^{2+}-dependent synaptotagmin−1 binding (Gerona *et al.*, 2000; Zhang *et al.*, 2002). The current results significantly extended this finding by revealing that the C-terminus of SNAP25 is a direct synaptotagmin−1 binding site and that the Ca^{2+}-dependent binding to

Table 1. Assignment of mass/charge peaks unique to C2AB-SNAP25 cross-linked products

			Cross-linked product			
			SNAP25		Synaptotagmin-1	
Observed mass	Expected mass	Ca^{2+}	Residues	Position	Residues	Position
1160.7	1161.4	+	177–184	C-term. SN2	K	β4 C2A
1669.6	1668.0	+	192–201	C-term. SN2	198–200	β4-loop 2 C2A
1685.9	1687.0	+	181–191	C-term. SN2	197–199	β4-loop 2 C2A
1696.8	1696.0	+	176–184	C-term. SN2	191–196	β4 C2A
2045.2	2045.0	±	32–40	N-term. SN1	289–297	β2-loop 1 C2B
1523.8	1522.5	−	77–83	C-term. SN1	191–196	β4 C2A
2468.5	2467.0	−	32–40	N-term. SN1	302–313	loop 1 C2B

the C-terminus of SNAP25 is mediated by basic β4-loop 2 C2A residues.

Two peaks with mass/charge ratios of 1523.8 and 2468.5 were observed only in the absence of Ca^{2+} (Table 1). The 1523.8 peak corresponded to synaptotagmin (191–196) cross-linked to SNAP25 (77–83). This cross-link represents an interaction between residues of C2A β4 with residues in the C-terminal portion of the N-terminal helix of SNAP25 (Figure 2). Combined with the preceding results, it was apparent that adjacent residues in the β4-loop 2 region of C2A shift their binding from C-terminal residues in the N-terminal helix (SN1) to C-terminal residues in the C-terminal helix (SN2) of SNAP25 when Ca^{2+} is bound (Figure 2). Thus, the β4-loop 2 region of C2A containing residues 191–200 operates as a Ca^{2+}-dependent switch for SNAP25 interactions.

Interactions of synaptotagmin C2B with SNAP25 were detected in the absence of Ca^{2+} (Table 1). The 2468.5 peak corresponded to synaptotagmin (301–313) cross-linked to SNAP25 (32–40). The 2045.2 peak was observed in both the presence or absence of Ca^{2+} (Table 1) that corresponded, respectively, to synaptotagmin (289–297) cross-linked to SNAP25 (32–40). Thus, this loop 1 region of C2B encompassing residues 289–313 engaged the N-terminal portion of the N-terminal helix of SNAP25 (SN1) in interactions in the absence of Ca^{2+} (Figure 2). In the presence of Ca^{2+}, the more N-terminal portion of the C2B loop 1 (residues 289-297) maintained SNAP25 binding, whereas SNAP25 binding by the C-terminal portion of the C2B loop 1 (residues 301-313) was not maintained in the presence of Ca^{2+} (Table 1). Because the C2B loop 1 contains Ca^{2+} ligands D303 and D309, Ca^{2+}-binding may directly occlude SNAP25 interactions with this region. Thus, C2B exhibited more subtle Ca^{2+}-dependent switching in its interactions with SNAP25 compared with that of C2A.

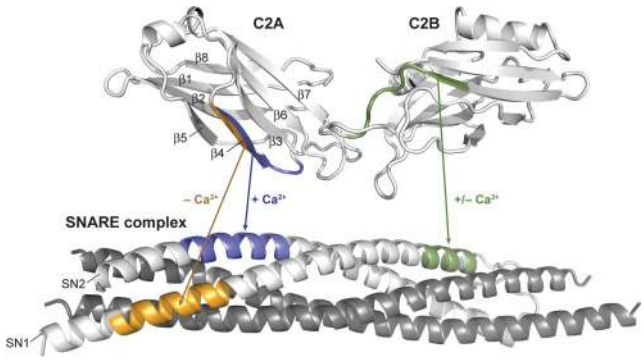

Figure 2. Schematic summary of C2AB interactions with SNAP25. The presence of Ca^{2+} altered interactions between C2A and C2B domains with SNAP25. For C2A, residues 191-196 bound the C terminal portion of the N terminal helix of SNAP25 (residues 77-83) in the absence but not presence of Ca^{2+} (orange). In the presence of Ca^{2+}, C2A residues 191–200 bound the C terminal helix of SNAP25 (residues 176-201; blue). For C2B, residues 301-313 bound to the N terminus of SNAP25 (residues 32-40; green) in the absence of Ca^{2+} but shifted to C2B residues 289-297 in the presence of Ca^{2+}.

The R199A/K200A Mutation Reduces Ca^{2+}-stimulated Synaptotagmin Binding to SNAREs

The Ca^{2+} switch region of C2A encompassing residues 191-200 that shifts interactions with SNAP25 upon Ca^{2+} binding consists of a positively charged region of C2A comprising β4-loop 2. To determine the importance of this C2A region for interactions with SNAP25, basic residues were mutated to alanine and effects on Ca^{2+}-dependent SNARE binding were determined. C2AB harboring R199A/K200A mutations was found to exhibit decreased (by 70%) Ca^{2+}-stimulated binding to immobilized ternary SNARE complexes (Figure 3a) and to SNAP25 but not to syntaxin (not shown). In contrast, Ca^{2+}-dependent SNARE binding of C2AB with E194A/K196A and K191A/K192A mutations was indistinguishable from wild-type C2AB (Figure 3a). These findings further refined the cross-linking results and indicated that R199 and K200 of the C2A loop 2 region are essential for Ca^{2+}-dependent synaptotagmin−1 binding. Significantly, the results also indicated that the same C2A residues important for Ca^{2+}-dependent binding to the C-terminus of SNAP25 were essential determinants for Ca^{2+}-dependent SNARE complex binding.

Mutations in Both C2A and C2B Eliminate SNARE Binding

C2A alone exhibited very limited Ca^{2+}-dependent SNAP25 and SNARE binding activity, which indicated an important contribution of C2B in the binding (Figure 1). Our cross-linking results revealed that C2B participated in SNAP25 interactions in both the absence and presence of Ca^{2+} (Table 1; Figure 2a). To assess the contribution of C2B residues to SNARE interactions in the presence of Ca^{2+}, C2AB harboring C2A and C2B mutations were tested for Ca^{2+}-dependent interactions with membrane-embedded heterodimeric SNARE complexes consisting of SNAP25 and syntaxin-1 (Figure 3b). Wild-type C2AB efficiently bound SNARE complexes reconstituted in PC liposomes in the presence of Ca^{2+} but not in its absence (Figure 3b). Confirming the previous binding studies, the R199A/K200A mutations in C2A reduced Ca^{2+}-

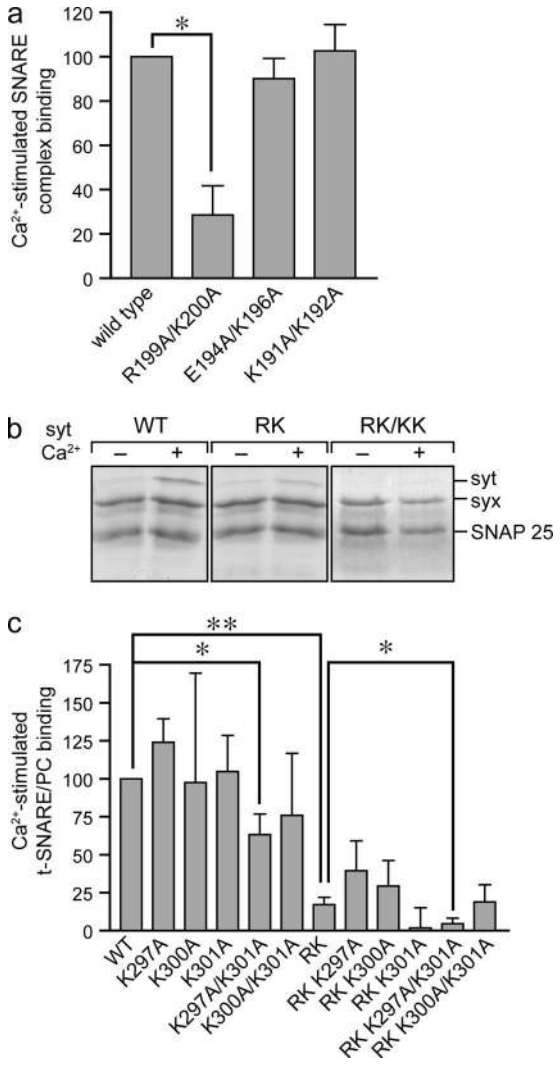

Figure 3. C2A loop 2 and C2B loop 1 mutations reduce Ca^{2+}-stimulated binding of C2AB to SNARE complexes. (a) Wild-type C2AB, C2AB(R199A/K200A), C2AB (E194A/K196A) or C2AB(K191A/K192A), all at 1 μM, were incubated with 1 μM SNARE complex immobilized on glutathione-Sepharose beads in the absence (−) or presence (+) of 1 mM $CaCl_2$. Binding of C2AB was determined by Western blotting after SDS PAGE. Mean values ± SE are shown (n = 3). (b) C2AB, C2AB(R199A/K200A) (RK) or C2AB (R199A/K200A/K297A/K301A) (RK/KK), all at 10 μM, were incubated with SNAP25/syntaxin-containing PC liposomes in the absence or presence of 1 mM Ca^{2+}. Liposome-bound C2AB was isolated from Accudenz gradients and analyzed by SDS-PAGE and Coomassie Blue staining. (c) C2AB and indicated mutants were incubated with SNAP25/syntaxin-containing liposomes in the presence or absence of 1 mM Ca^{2+}. RK corresponds to R199A/K200A. Bound C2AB was analyzed as in panel b, quantified by densitometry, and normalized to syntaxin in each gradient. Ca^{2+}-dependent binding by C2AB mutants was expressed as the difference bound in the presence or absence of Ca^{2+} and normalized to binding by wild-type C2AB. Mean values ± SE are shown (n = 3). Differences in binding between wild-type C2AB and RK or K297A/K301A mutants, or between RK and RK/K297A/K301A mutants were significant (**$p < 0.01$; *$p < 0.05$).

dependent binding of C2AB by 5.7-fold (Figure 3, b and c). C2B mutations individually had, in most cases, little effect on Ca^{2+}-dependent SNARE binding although binding by C2AB harboring K297A/K301A mutations was significantly reduced (Figure 3c). However, when the C2B (K297A/K301A) mutations were combined with the C2A (R199A/K200A) mutations, there was a virtually complete (22-fold decrease) loss of Ca^{2+}-dependent SNARE binding (Figure 3, b and c). The loss of Ca^{2+}-dependent binding by the double mutant C2AB confirmed the results of the cross-linking and indicated the participation of both C2 domains for SNARE binding in the presence of Ca^{2+}.

SNARE-binding Mutations in C2AB Do Not Affect Ca^{2+}-dependent PS or PIP_2 Interactions

Ca^{2+}-dependent PS binding is the major biochemical activity of synaptotagmin−1 that has been implicated in Ca^{2+}-coupling to membrane fusion (Geppert *et al.*, 1994; Littleton *et al.*, 1994; Zhang *et al.*, 1998). The Ca^{2+}-dependent SNARE-binding loop 2 of C2A is sufficiently distant from the PS-binding residues in loops 1 and 3 to allow for simultaneous PS and SNARE binding, which has been reported (Davis *et al.*, 1999; but see Arac *et al.*, 2003 for a different view). We directly assessed whether loop 2 residues were important for Ca^{2+}-dependent PS-binding by conducting binding studies with PC/PS (85:15) liposomes. Wild-type C2AB exhibited Ca^{2+}-dependent binding to PC/PS liposomes, but not to liposomes containing PC (not shown), with an EC_{50} = 182 ± 21 μM Ca^{2+} (±SE, n = 3; Figure 4a). Indistinguishable Ca^{2+}-dependent binding to PC/PS liposomes was observed for C2AB (R199A/K200A) as well as for C2AB (R199A/K200A/K297A/K301A), which exhibited EC_{50} values of 155 ± 8 and 211 ± 34 μM Ca^{2+} (±SE, n = 3), respectively. Similarly, wild-type and mutant C2AB were found to exhibit indistinguishable Ca^{2+}-dependent binding to PC/PIP_2 liposomes (Figure 4b). These results indicated that these residues in C2A loop 2 and C2B loop 1 are not required for Ca^{2+}-dependent interactions of synaptotagmin−1 with phospholipid bilayers containing PS or PIP_2. In contrast, C2AB (R199A/K200A) as well as C2AB (R199A/K200A/K297A/K301A) mutants exhibited markedly impaired Ca^{2+}-dependent binding to SNARE complexes embedded in PC-containing liposomes (Figure 4c). Thus, mutations in C2A and C2B that abrogated Ca^{2+}-dependent SNARE binding did not affect Ca^{2+}-dependent PS or PIP_2 binding. Synaptotagmin point mutants with this selectivity have not previously been generated and provide a unique opportunity to assess the functional role of Ca^{2+}-dependent SNARE binding.

C2A Loop 2 Mutations Eliminate C2AB-mediated Ca^{2+} Stimulation of SNARE-dependent Liposome Fusion

Synaptotagmin C2AB confers Ca^{2+} stimulation on SNARE-dependent liposome fusion in vitro (Tucker *et al.*, 2004). We used the liposome fusion assay to characterize C2AB mutants that were selectively impaired in Ca^{2+}-dependent SNARE binding. Wild-type C2AB stimulated SNARE-mediated liposome fusion in the presence of Ca^{2+} by enhancing both its rate and extent (Figure 5a) as reported (Tucker *et al.*, 2004). In the absence of Ca^{2+}, C2AB reproducibly inhibited liposome fusion, possibly due to Ca^{2+}-independent SNARE binding. C2AB with a single mutation in C2B (K297A), which exhibited wild-type Ca^{2+}-dependent SNARE binding (Figure 3c), was also fully capable of mediating Ca^{2+}-stimulated liposome fusion (Figure 5b). In contrast, C2AB with two mutations in C2B (K297A/K301A), which exhibited partial impairment (~40%) of Ca^{2+}-dependent SNARE binding (Figure 3c), showed partially reduced activity in the liposome fusion assay (Figure 5b). C2AB with mutations in C2A exhibited a much stronger loss of function in the fusion assay. Thus, C2AB (R199A/K200A) was completely inactive

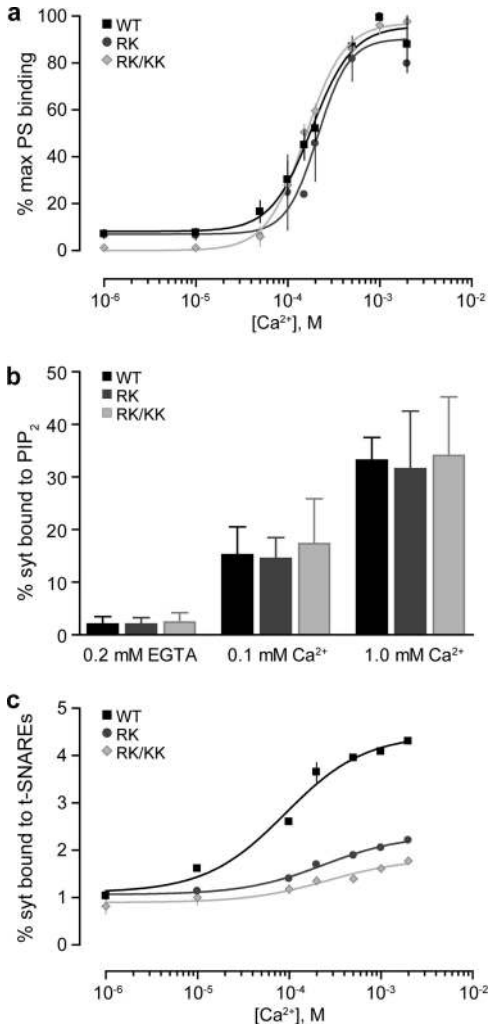

Figure 4. C2A loop 2 and C2B loop 1 mutants exhibit decreased Ca^{2+}-dependent SNARE binding but normal Ca^{2+}-dependent phosphatidylserine binding. (a) C2AB, C2AB(R199A/K200A) (RK) or C2AB(R199A/K200A/K297A/K301A) (RK/KK) were incubated with protein-free PC liposomes containing 15% PS at the indicated Ca^{2+} concentrations and bound C2AB was determined as in Figure 3b. Maximal bound C2AB was set equal to 100% and plotted (±SE, n = 3) as a function of [Ca^{2+}]. (b) C2AB, C2AB(R199A/K200A) (RK), or C2AB(R199A/K200A/K297A/K301A) (RK/KK) were incubated with protein-free PC liposomes containing 5% PIP_2 at the indicated Ca^{2+} concentrations and bound C2AB was determined as in Figure 3b. Fractional bound C2AB was plotted (±SE, n = 3) as a function of [Ca^{2+}]. (c) C2AB and indicated mutants were incubated with PC liposomes containing SNARE complexes at the indicated Ca^{2+} concentrations, and bound C2AB was determined as in Figure 3b. The fraction of C2AB bound was plotted (±SE, n = 3) as a function of [Ca^{2+}].

in mediating Ca^{2+}-stimulated liposome fusion (Figure 5c), which corresponded to its strong loss of Ca^{2+}-dependent SNARE binding (Figure 3c). C2AB with mutations in both C2A (R199A/K200A) and C2B (K297A/K301A), which exhibited virtually no Ca^{2+}-stimulated SNARE binding (Figure 3c), was completely inactive in mediating Ca^{2+}-stimulated liposome fusion (Figure 5c). Overall, loss of function in the liposome fusion assay by C2AB (Figure 5) correlated with reduced Ca^{2+}-dependent SNARE binding (Figure 3c). The data indicate that Ca^{2+}-dependent SNARE binding by C2AB is required to mediate the Ca^{2+} stimulation of SNARE-dependent liposome fusion, which is consistent with the conclusions of a recent study (Bhalla *et al.*, 2006).

Because the biochemical properties of synaptotagmin−1 exhibit diverse Ca^{2+}-dependencies, we examined the Ca^{2+}-dependence of liposome fusion promoted by wild-type and mutant C2AB proteins. Wild-type C2AB conferred Ca^{2+} stimulation with an EC_{50} = 113 ± 4 μM Ca^{2+} (±SE, n = 3; Figure 5d). In contrast, C2AB harboring C2A (R199A/K200A) mutations significantly shifted the Ca^{2+} dose response to the right with an EC_{50} = 181 ± 9 μM Ca^{2+} (±SE, n = 3). C2AB harboring both C2A (R199A/K200A) and C2B (K297A/K301A) mutations exhibited the same shifted EC_{50} = 187 ± 9 μM Ca^{2+} (±SE, n = 3). The results indicated that impaired Ca^{2+}-dependent SNARE binding by C2A loop 2 mutants altered the coupling between Ca^{2+} and membrane fusion in vitro.

Synaptotagmin−1 C2A Loop 2 Mutations Fail to Mediate Ca^{2+}-triggered Vesicle Exocytosis in PC12 Cells

The preceding results established that C2A (R199A/K200A) and C2B (K297A/K301A) mutations in synaptotagmin−1 selectively abolish Ca^{2+}-dependent SNARE binding without affecting Ca^{2+}-dependent PS or PIP_2 binding. This provided the opportunity to determine the role of Ca^{2+}-dependent SNARE binding in the function of synaptotagmin−1 in cells. Synaptotagmins-1 and -9 mediate the Ca^{2+}-triggering of vesicle exocytosis in PC12 cells. The concomitant shRNA-mediated down-regulation of both isoforms results in a complete block in Ca^{2+}-triggered vesicle exocytosis at a step following vesicle docking (Lynch and Martin, 2007). Expression of either synaptotagmin with silent mutations that bypass the shRNA targeting fully restores Ca^{2+}-dependent vesicle exocytosis in the synaptotagmin−1/9-null PC12 cells (Lynch and Martin, 2007). Thus, we tested synaptotagmin−1 rescue constructs that encode C2A (R199A/K200A) or C2A (R199A/K200A) plus C2B (K297A/K301A) mutants. Wild-type and mutant synaptotagmins were expressed in the synaptotagmin−1/9-null PC12 cells at levels comparable (30–50%) to that in wild-type PC12 cells, which was proportional to transfection efficiency (Figure 6a). Expressed wild-type and mutant synaptotagmins were each correctly trafficked to dense-core vesicles as shown by colocalization with the dense-core vesicle content protein chromogranin B (Figure 6b). Thus, these mutations did not affect protein expression levels or proper targeting of the proteins to dense-core vesicles.

To monitor regulated exocytosis in PC12 cells, we coexpressed a prepro atrial natriuretic peptide-EGFP (ANF-EGFP), which is sorted to dense-core vesicles in wild-type and in synaptotagmin-depleted PC12 cells (Lynch and Martin, 2007). ANF-EGFP was properly targeted to dense-core vesicles in cells that re-expressed wild-type and mutant synaptotagmins (see Supplementary Figure S1). Incubation in depolarizing high K^+ buffer was used to promote Ca^{2+} influx and trigger vesicle exocytosis, which was detected as single exocytic events by TIRF microscopy. The time course of averaged cumulative fusion events over the first 60 s of incubation in high K^+ buffer revealed that wild-type PC12 cells exhibited 17.6 ± 2.5 (±SE, n = 25) events (Figure 6c). In contrast, synaptotagmin−1/9-null cells exhibited 0.5 ± 0.1 (±SE, n = 25) events (Figure 6c), confirming the requirement for synaptotagmin in Ca^{2+}-triggered dense-core vesicle exocytosis (Lynch and Martin, 2007). Synaptotagmin−1 expression in synaptotagmin-null cells fully restored Ca^{2+}-triggered vesicle exocytosis with an average of 14.6 ± 1.8 (±SE, n = 20) fusion events in 60 s (Figure 6c). In contrast, expression of synaptotagmin−1 with C2A (R199A/K200A) muta-

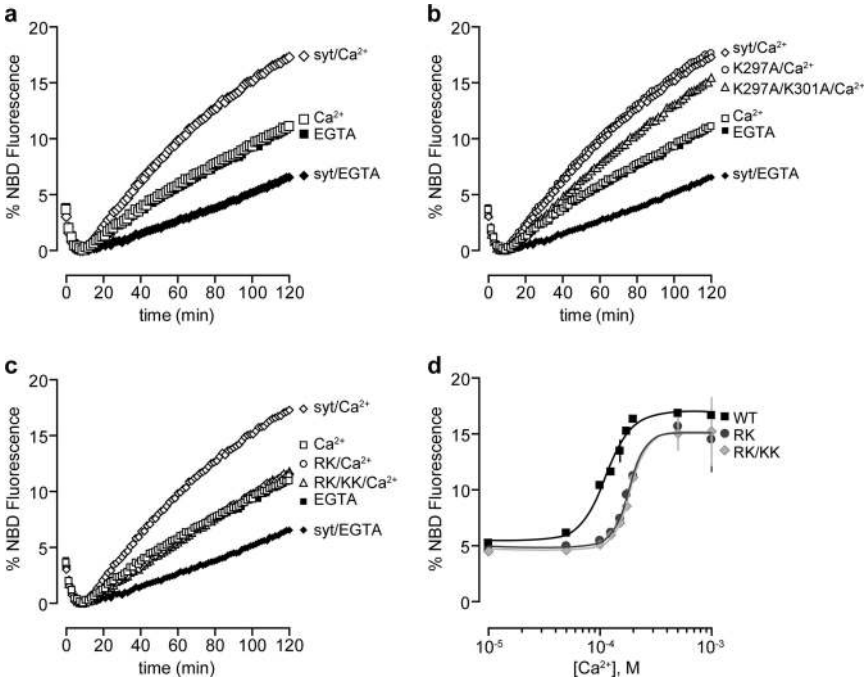

Figure 5. C2A loop 2 and C2B loop 1 mutations reduce Ca^{2+} stimulation of liposome fusion mediated by C2AB. (a) C2AB, 10 μM, stimulated the fusion of v-SNARE with t-SNARE liposomes in the presence of 100 μM Ca^{2+} but not in the presence of 0.2 mM EGTA. NBD fluorescence was expressed as percentage maximum fluorescence after 1% dodecyl maltoside addition. (b) C2AB, C2AB(K297A), or C2AB(K297A/K301A), all at 10 μM, were tested in the liposome fusion assay. C2AB(K297A/K301A) exhibited partial loss of function in conferring Ca^{2+} stimulation. (c) C2AB(R199A/K200A) (RK) or C2AB (R199A/K200A/K297A/K301A) (RK/KK) mutants failed to stimulate liposome fusion in the presence of 100 μM Ca^{2+}. (d) C2AB, 10 μM, and mutants were incubated in the liposome fusion assay with indicated [Ca^{2+}]. % maximal NBD fluorescence at 120 min was plotted as a function of [Ca^{2+}] ($\pm$SE, n = 3). EC_{50} values for Ca^{2+} were 113 μM ($\pm$4 μM) for C2AB, 181 μM ($\pm$9 μM) for C2AB(R199A/K200A) (RK), and 187 μM ($\pm$9 μM) for C2AB (R199A/K200A/K297A/K301A) (RK/KK).

tions only partially restored Ca^{2+}-triggered exocytosis, with only 4.3 $\pm$ 0.1 ($\pm$SE, n = 15) fusion events observed in 60 s (Figure 6c). Expression of synaptotagmin−1 containing both C2A (R199A/K200A) and C2B (K297A/K301A) mutations entirely failed to restore Ca^{2+}-triggered exocytosis (0.4 $\pm$ 0.2 fusion events, $\pm$SE, n = 15; Figure 6c). The results indicated that mutant synaptotagmin−1, which is selectively impaired for Ca^{2+}-dependent SNARE binding, but not for Ca^{2+}-dependent PS or PIP_2 binding, exhibits strong to complete loss-of-function in Ca^{2+}-triggered exocytosis in proportion to the extent of SNARE-binding defects. We conclude that Ca^{2+}-dependent SNARE binding is essential for synaptotagmin−1 function as a Ca^{2+} sensor that regulates fusion probabilities.

A Model for Ca^{2+}-dependent Synaptotagmin C2A Function

Although NMR and crystal structures for synaptotagmin and SNARE complexes have been solved (Sutton *et al.*, 1995, 1998, 1999; Shao *et al.*, 1998; Fernandez *et al.*, 2001), structures of synaptotagmin-bound SNARE complexes are not yet available. To predict the structure of a Ca^{2+}-dependent complex between the C2A loop 2 region of synaptotagmin−1 and the C-terminus of SNAP25 in the SNARE complex, we used the ZDOCK program (Chen and Weng, 2002; Chen *et al.*, 2003) and available structures of C2A and SNARE complexes.

An initial set of 40,000 binding complexes was generated by systematically docking the atomic coordinates of the SNARE complex to each of 20 NMR structures of the C2A domain. To predict complexes that represented the Ca^{2+}-dependent interaction between C2A and SNAP25, we set restraints on the docking experiment. Our previous studies, confirmed by the cross-linking results, showed that three acidic residues in the C-terminus of SNAP25 (D179, D186, D193) are essential for Ca^{2+}-dependent interactions between synaptotagmin−1 and SNARE complexes (Zhang *et al.*, 2002). Fifty-nine docked complexes were identified in which C2A residues were within 5 Å of the three acidic residues of SNAP25. Complexes with C2A loop 2 residues K196, R199, and K200 in proximity to the three acidic residues in SNAP25 were found to be most prevalent (Figure 7a). We performed a complementary docking experiment in which C2A R199 and K200 residues were used as reference points to identify complexes with SNAP25 that were within 5 Å. Only 28 complexes were generated that satisfied this restraint, and three of these coincided with complexes from the first docking experiment. One of this set of three complexes is depicted in Figure 7b.

Because ZDOCK uses a soft docking protocol, not all complexes identified are energetically favorable. Thus, we scored complexes from the docking experiments by assessing binding energies. Total binding energy for each complex was calculated using the DoME program (Marcia *et al.*, 2005) taking electrostatic and van der Waals potentials into account. Few of the docked complexes exhibited binding energies < -10 kcal/mol, which would be required to overcome entropy loss upon complexation (Erickson, 1989). The complex depicted in Figure 7b exhibited the second lowest or lowest binding energy calculated for the first or second docking experiments, respectively (Supplementary Tables S1 and S2; complex 1–1826), which was calculated as −18.09 kcal/mol. Thus, this complex (Figure 7b) represented the most stable docking orientation for Ca^{2+}-dependent synaptotagmin−1–SNARE interactions that satisfied constraints based on the cross-linking and mutagenesis studies. The predicted complex showed close proximity of the C-terminal acidic residues in SNAP 25 (D179, D186, D193) with the cluster of basic residues in C2A β4-loop 2 (K196, R199, K200). Mutation of C2A R199 and K200 to alanine was calculated to destabilize this complex by converting its total binding energy to a more positive value.

The cluster of basic residues in C2A loop 2 (K196, R199, K200) is orthogonal to the membrane-penetrating face of C2A containing residues M173 and F234 in loops 1 and 3, respectively (Figure 8a). Thus, it was possible to model Ca^{2+}-bound C2A in energetically favorable SNARE inter-

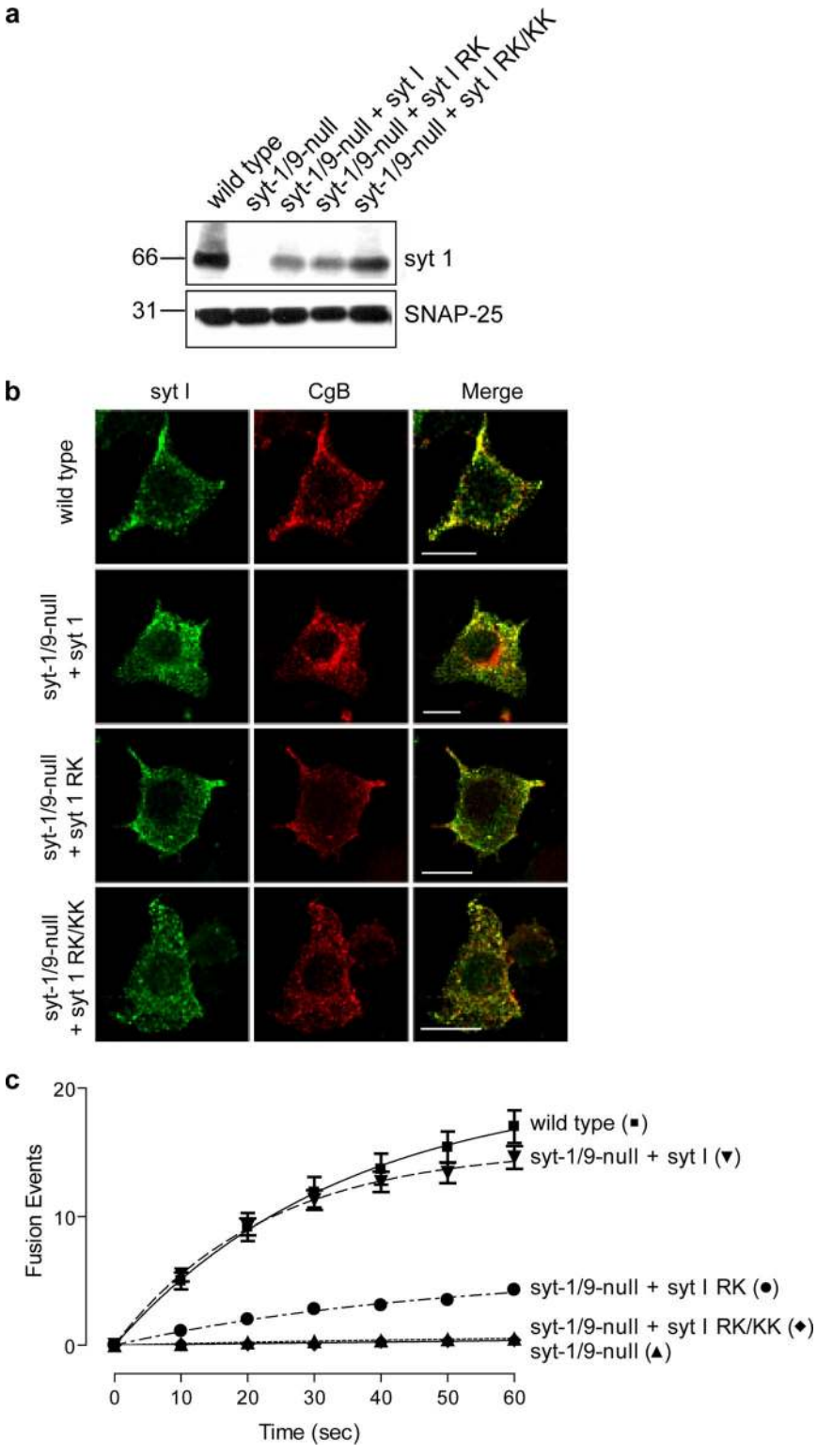

Figure 6. Synaptotagmin−1 mutants fail to restore Ca^{2+}-dependent exocytosis in synaptotagmin-depleted PC12 cells. (a) Immunoblot analysis of wild-type PC12 cells, synaptotagmin−1/9-null cells, and null cells expressing wild-type synaptotagmin−1 or R199A/K200A (RK) or R199A/K200A/K297A/K301A (RK/KK) mutants. SNAP25 was used as a loading control. (b) Wild-type and synaptotagmin−1/9-null cells expressing synaptotagmin−1 or indicated mutants were fixed and stained with synaptotagmin−1 (green channel) and CgB (red channel) antibodies, and colocalization was determined (yellow). The synaptotagmin−1 mutants were localized to dense-core vesicles. (c) Cells expressing ANF-EGFP were stimulated with depolarization medium, and images were acquired at 0.25-s intervals. Fusion events were counted as a flash/puff of fluorescence for each cell type, and the sum of fusion events in 10-s intervals was determined. The sums of the average number of fusion events per cell over time (mean value ± SD) for wild-type (n = 25), synaptotagmin−1/9-null (n = 25), synaptotagmin−1/9-null + synaptotagmin−1 (n = 20), synaptotagmin−1/9-null + synaptotagmin−1 RK (n = 15), and synaptotagmin−1/9-null + synaptotagmin−1 RK/KK (n = 15) cells were plotted.

actions while simultaneously penetrating the membrane (Figure 8b).

DISCUSSION

Synaptotagmins are essential for Ca^{2+}-triggered vesicle exocytosis (Littleton *et al.*, 1993; Nonet *et al.*, 1993; Geppert *et al.*, 1994; Lynch and Martin, 2007) and function as Ca^{2+} sensors for regulated vesicle fusion (Brose *et al.*, 1992; Geppert *et al.*, 1994). However, the precise mechanism used by synaptotagmins for coupling Ca^{2+} rises to vesicle exocytosis has been unclear (Chapman, 2002; Sudhof, 2002; Rizo *et al.*, 2006). The current work provides the first direct in vivo evidence that synaptotagmin−1 functions as a Ca^{2+} sensor by binding to

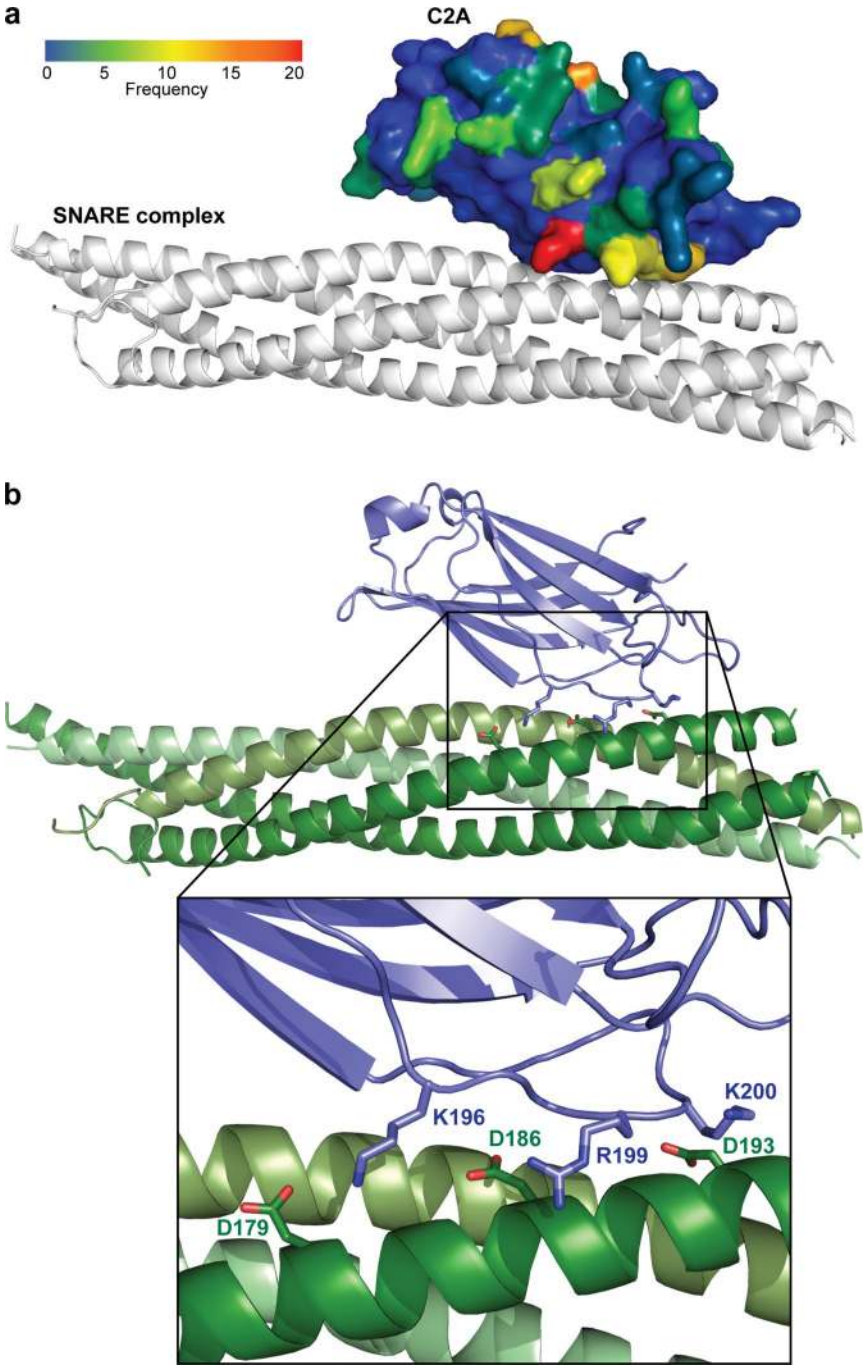

Figure 7. Ca^{2+}-dependent C2A/SNARE binding interface derived from computational modeling. (a) Using ZDOCK, each of 20 NMR structures of C2A was computationally docked to the atomic coordinates of the SNARE complex crystal structure. The frequency of occurrence of individual C2A residues within 5 Å of acidic C-terminal SNAP25 residues D179, D186, and D193 is depicted. C2A is shown in a space filling model docked to a ribbon model of the SNARE complex. C2A residues are colored according to their frequency of proximity to SNAP25 D179, D186, or D193 from 0 (blue) to 20 (red) of 59. (b) The model shows the predicted low-energy docking orientation for Ca^{2+}-dependent C2A-SNARE binding. The model corresponds to complex 1–1826 shown in Supplementary Tables S1 and S2. Close-up view depicts the binding interface for synaptotagmin−1 residues (K196, R199, and K200) with SNAP 25 residues (D179, D186, and D193).

the membrane fusion machinery comprised of SNARE proteins. These studies identified a unique surface on synaptotagmin−1 C2A comprised of loop 2 basic residues that mediate Ca^{2+}-dependent interactions with SNARE complexes in Ca^{2+}-triggered vesicle exocytosis.

Ca^{2+}-dependent interactions of synaptotagmin−1 with individual SNARE proteins and SNARE complexes in vitro have been extensively characterized because such interactions provide an attractive mechanism by which Ca^{2+} rises could be coupled directly to membrane fusion (Chapman *et al.*, 1995; Li *et al.*, 1995; Kee and Scheller, 1996; Davis *et al.*, 1999; Gerona *et al.*, 2000; Zhang *et al.*, 2002). However, the physiological role of SNARE binding by synaptotagmin−1 had not been directly assessed because of the lack of precise point mutations that selectively eliminate Ca^{2+}-dependent SNARE binding. Our cross-linking studies identified residues in the β4-loop 2 region of C2A that comprise a Ca^{2+}-dependent switch for synaptotagmin−1 C2A interactions with SNAREs. In the presence of Ca^{2+}, C2A loop 2 basic residues interact with acidic residues in the C-terminus of SNAP25, which is highly significant because this region of SNAP25 is essential for the Ca^{2+} regulation of vesicle exocytosis (Gerona *et al.*, 2000; Zhang *et al.*, 2002). The current work revealed that these C-terminal residues of SNAP25 comprise a direct site for Ca^{2+}-dependent binding of synaptotagmin−1 to SNARE complexes.

The C2A loop 2 has not been previously implicated in the biochemical properties of synaptotagmin−1. An R199Q mu-

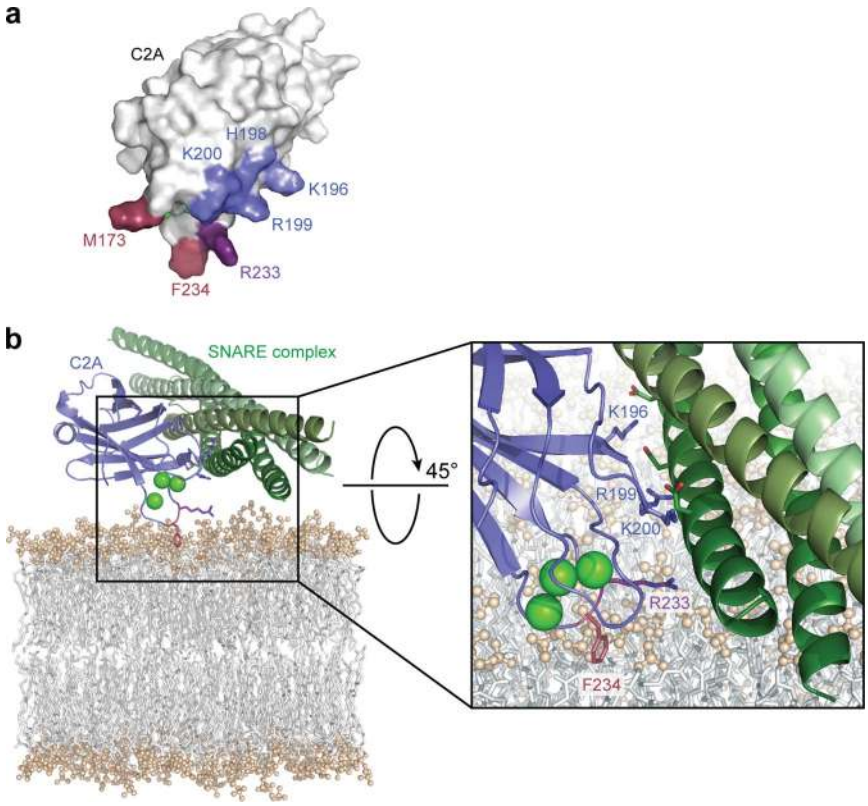

Figure 8. Membrane-docked model for Ca^{2+}-dependent C2A-SNARE interaction. (a) Space-filling model of C2A depicting clustered basic residues of β4-loop 2 (K196, H198, R199, and K200) positioned orthogonally to membrane-inserting (M173 and F234) residues of loops 1 and 3. R233 is shown as positioned between both interfaces. (b) Model depicts simultaneous interactions of C2A with SNARE complex and membrane. Ca^{2+} ions (green spheres) bound by loops 1 and 3 with F234 penetrating the bilayer are shown. The orthogonal face containing K196, R199, and K200 interacting with SNAP25 C-terminal helix is depicted. R233 is shown between membrane- and SNARE-binding interfaces.

tation was reported to have little effect on either PS or syntaxin binding (Shao *et al.*, 1997; Zhang *et al.*, 1998). The R199/K200 residues that mediate Ca^{2+}-dependent SNARE binding reside at the apex of loop 2 in proximity to Ca^{2+}-binding ligands on loops 1 and 3. R199 and K200 along with H198 and K196 form a positively charged cluster (see Figure 8a). Because Ca^{2+} binding does not cause a significant conformational change in C2A (Shao *et al.*, 1996), it is thought that Ca^{2+}-dependent effector binding by C2A is driven by nonspecific electrostatic interactions triggered by Ca^{2+} binding (Shao *et al.*, 1997; Rizo and Sudhof, 1998). Ca^{2+} neutralizes acidic residues in loops 1 and 3 to shift the surface of C2A from a negative to positive electrostatic potential. This model has been successfully applied to understanding how Ca^{2+} binding drives the initial association of basic residues such as R233 (Zhang *et al.*, 1998; Fernandez-Chacon *et al.*, 2001) in C2A with negatively charged membranes (Murray and Honig, 2002). We propose that ligation of Ca^{2+} by loop 1 and 3 residues would shift the surface of C2A to a positive electrostatic potential that facilitates binding of R199 and K200 (and probably K196 and H198) to acidic residues in the C terminus of SNAP25. An electrostatic switch would enable rapid Ca^{2+}-triggered binding kinetics as has been observed for synaptotagmin−1 interactions with SNAP25 in vitro (Bai *et al.*, 2004).

Our model for synaptotagmin−1 interactions with SNAREs (Figure 8b) clarifies an important aspect of the Ca^{2+}-regulated function of C2A by revealing that simultaneous interactions with anionic phospholipid membranes and SNARE complexes are feasible. Concomitant binding was demonstrated in one in vitro study (Davis *et al.*, 1999) but not in another (Arac *et al.*, 2003). In the absence of anionic phospholipids, three Ca^{2+} ions bind to C2A only at high [Ca^{2+}] well beyond the intracellular physiological range (Ubach *et al.*, 1998; Fernandez-Chacon *et al.*, 2001). In the presence of anionic phospholipid membranes, affinities for Ca^{2+} binding to C2A increase up to 5000-fold (Zhang *et al.*, 1998) bringing the effective [Ca^{2+}] for binding into the intracellular physiological range. SNARE binding by synaptotagmin−1 can also be driven by Ca^{2+} in the absence of phospholipids but the affinities for Ca^{2+} are very low (~100 μM) (Figure 4b), which contrasts sharply with Ca^{2+} concentrations (1–10 μM) that promote synaptotagmin−1 cross-linking to SNAP25 and trigger vesicle exocytosis in PC12 cells (Zhang *et al.*, 2002). Ca^{2+}-dependent SNARE binding by synaptotagmin−1 would likely not be achieved at intracellular Ca^{2+} concentrations in the absence of accompanying phospholipid binding. As our model shows (Figure 8a), the basic cluster of C2A loop 2 residues (K196, H198, R199, K200) is positioned orthogonally to loop 1 and loop 3 Ca^{2+}-binding and membrane-inserting residues, which would allow simultaneous interactions with the SNAP25 C terminus in the SNARE complex and with the membrane. R233 is positioned at both SNAP25- and membrane-binding interfaces (Figure 8b), which accounts for the finding that C2A R233Q mutations decrease both Ca^{2+}-dependent anionic membrane as well as SNAP25 interactions but not those with syntaxin (Fernandez-Chacon *et al.*, 2001; Wang *et al.*, 2003).

Cross-linking revealed that the C2B domain of synaptotagmin−1 also contributed to SNAP25 binding in the presence of Ca^{2+}. We found that C2B loop 1 mutations partially reduced Ca^{2+}-dependent binding of synaptotagmin−1 to SNARE complexes but fully (> 95%) abolished binding when combined with C2A loop 2 mutations. These studies revealed a requirement for both C2A and C2B domain residues in Ca^{2+}-dependent interactions with SNAREs, which is consistent with previous findings that neither C2A nor C2B fragments possess full Ca^{2+}-dependent SNARE-binding activity (Davis *et al.*, 1999; Gerona *et al.*, 2000), that Ca^{2+} ligand mutations in both C2 domains are needed to elimi-

nate Ca^{2+}-dependent SNARE binding (Earles *et al.,* 2001) and that lengthening the linker between C2 domains reduces Ca^{2+}-dependent SNARE binding (Bai *et al.,* 2004). Unfortunately because of the limited information available, we were unable to model C2B interactions with SNAREs.

In vitro binding studies with C2A loop 2 and C2B loop 1 mutants revealed that these mutations result in a selective loss of Ca^{2+}-dependent SNARE binding without affecting Ca^{2+}-dependent PS or PIP_2 binding. No other defined point mutants in synaptotagmin−1 with these selective properties have been described although synaptotagmin−1 with inter-C2 domain linker extensions exhibit similar but attenuated properties (Bai *et al.,* 2004). The selective loss of Ca^{2+}-dependent SNARE binding by the C2A and C2B mutants provided the opportunity to critically assess this property of synaptotagmin−1 for its function as a Ca^{2+} sensor in regulated vesicle exocytosis. We found that the synaptotagmin−1 C2A (R199A/K200A) mutant was strongly impaired in restoring Ca^{2+}-dependent exocytosis in synaptotagmin−1/9-null PC12 cells and that the C2A (R199A/K200A) C2B (K297A/K301A) double mutant was completely nonfunctional. Because both mutants were normally expressed and properly targeted to dense-core vesicles, these results provide unambiguous evidence for the essential role of Ca^{2+}-dependent SNARE binding for synaptotagmin−1 function in regulated exocytosis. Moreover, they indicate that Ca^{2+}-dependent interactions of synaptotagmin−1 with membranes are insufficient in the absence of SNARE binding to trigger fusion. The results highlight important roles for both C2 domains in function, which is consistent with previous genetic studies of synaptotagmin−1 in Ca^{2+}-triggered vesicle exocytosis (Yoshihara *et al.*, 2003). Particularly relevant is the observation that a C2A Ca^{2+} ligand mutation D232N increases the Ca^{2+} sensitivity of neurotransmitter release and the Ca^{2+}-dependent binding of synaptotagmin−1 to SNAREs (Stevens and Sullivan, 2003; Pang *et al.*, 2006), which is in accord with our conclusion that C2A contains a Ca^{2+}-dependent switch for SNARE binding.

Although the current work provides important new insights on SNARE regulation by synaptotagmin−1 in Ca^{2+}-triggered vesicle exocytosis, the precise role of Ca^{2+}-dependent SNARE interactions remains to be clarified. Synaptotagmin−1 may function at an early stage to recruit SNAP25 into SNARE complexes for assembly of fusogenic SNARE complexes (Bhalla *et al.,* 2006; Chen *et al.,* 2001). Alternatively, a later-stage role for Ca^{2+}-dependent synaptotagmin−1 binding to SNAP25 may be to displace SNARE complex-bound complexin, which could drive SNARE complexes into executing fusion (Reim *et al.,* 2001; Tokumaru *et al.,* 2001; Chen *et al.,* 2002; Giraudo *et al.,* 2006; Schaub *et al.,* 2006; Tang *et al.,* 2006). The Ca^{2+}-dependent binding of C2A loop 2 of synaptotagmin−1 to C-terminal SNAP25-containing complexes may be well positioned to execute complexin displacement for triggering fusion.

In summary, the current work identified surfaces on the C2A and C2B domains of synaptotagmin−1 that mediate Ca^{2+}-dependent binding to SNAP25 in SNARE complexes. Mutation of basic residues on these surfaces abrogate Ca^{2+}-dependent interactions with SNARE complexes and abrogate Ca^{2+}-triggered vesicle exocytosis without affecting Ca^{2+}-dependent membrane binding. The results provide strong evidence that 1) Ca^{2+}-dependent membrane interactions alone are insufficient for mediating the function of synaptotagmin−1 and 2) that the Ca^{2+} sensing role of synaptotagmin−1 in regulating vesicle exocytosis requires its direct interaction with the SNARE fusion machinery.

ACKNOWLEDGMENTS

The authors thank Adam Steinberg for creating the model figures. This work was supported by US Public Health Service Grant DK25861 to T.F.J.M., by a Ruth L. Kirschstein predoctoral fellowship to K.L.L., by Department of Energy-Genomics to Life Grant DE-FG02-04ER25627 to J.C.M., and by support of R.F.M. by National Library of Medicine Grant 5T15LM007359-03.

REFERENCES

Arac, D., Murphy, T., and Rizo, J. (2003). Facile detection of protein-protein interactions by one-dimensional NMR spectroscopy. Biochemistry *42*, 2774–2780.

Bai, J., Wang, C. T., Richards, D. A., Jackson, M. B., and Chapman, E. R. (2004). Fusion pore dynamics are regulated by synaptotagmin*t-SNARE interactions. Neuron *41*, 929–942.

Bai, J., Wang, P., and Chapman, E. R. (2002). C2A activates a cryptic Ca^{2+}-triggered membrane penetration activity within the C2B domain of synaptotagmin I. Proc. Natl. Acad. Sci. USA *99*, 1665–1670.

Bennett, M. K., Calakos, N., and Scheller, R. H. (1992). Syntaxin: a synaptic protein implicated in docking of synaptic vesicles at presynaptic active zones. Science *257*, 255–259.

Bhalla, A., Chicka, M. C., Tucker, W. C., and Chapman, E. R. (2006). Ca^{2+}-synaptotagmin directly regulates t-SNARE function during reconstituted membrane fusion. Nat. Struct. Mol. Biol. *13*, 323–330.

Bhalla, A., Tucker, W. C., and Chapman, E. R. (2005). Synaptotagmin isoforms couple distinct ranges of Ca^{2+}, Ba^{2+}, and Sr^{2+} concentration to SNARE-mediated membrane fusion. Mol. Biol. Cell *16*, 4755–4764.

Brose, N., Petrenko, A. G., Sudhof, T. C., and Jahn, R. (1992). Synaptotagmin: a calcium sensor on the synaptic vesicle surface. Science *256*, 1021–1025.

Chapman, E. R. (2002). Synaptotagmin: a Ca^{2+} sensor that triggers exocytosis? Nat. Rev. Mol. Cell Biol. *3*, 498–508.

Chapman, E. R., Desai, R. C., Davis, A. F., and Tornehl, C. K. (1998). Delineation of the oligomerization, AP-2 binding, and synprint binding region of the C2B domain of synaptotagmin. J. Biol. Chem. *273*, 32966–32972.

Chapman, E. R., Hanson, P. I., An, S., and Jahn, R. (1995). Ca^{2+} regulates the interaction between synaptotagmin and syntaxin 1. J. Biol. Chem. *270*, 23667–23671.

Chen, R., Li, L., and Weng, Z. (2003). ZDOCK: an initial-stage protein-docking algorithm. Proteins *52*, 80–87.

Chen, R., and Weng, Z. (2002). Docking unbound proteins using shape complementarity, desolvation, and electrostatics. Proteins *47*, 281–294.

Chen, X., Tomchick, D. R., Kovrigin, E., Arac, D., Machius, M., Sudhof, T. C., and Rizo, J. (2002). Three-dimensional structure of the complexin/SNARE complex. Neuron *33*, 397–409.

Chen, Y. A., Scales, S. J., Jagath, J. R., and Scheller, R. H. (2001). A discontinuous SNAP-25 C-terminal coil supports exocytosis. J. Biol. Chem. *276*, 28503–28508.

Davis, A. F., Bai, J., Fasshauer, D., Wolowick, M. J., Lewis, J. L., and Chapman, E. R. (1999). Kinetics of synaptotagmin responses to Ca^{2+} and assembly with the core SNARE complex onto membranes. Neuron *24*, 363–376.

Douglas, W. W., and Rubin, R. P. (1961). The role of calcium in the secretory response of the adrenal medulla to acetylcholine. J. Physiol. *159*, 40–57.

Earles, C. A., Bai, J., Wang, P., and Chapman, E. R. (2001). The tandem C2 domains of synaptotagmin contain redundant Ca^{2+} binding sites that cooperate to engage t-SNAREs and trigger exocytosis. J. Cell Biol. *154*, 1117–1123.

Erickson, H. P. (1989). Co-operativity in protein-protein association. The structure and stability of the actin filament. J. Mol. Biol. *206*, 465–474.

Ernst, J. A., and Brunger, A. T. (2003). High resolution structure, stability, and synaptotagmin binding of a truncated neuronal SNARE complex. J. Biol. Chem. *278*, 8630–8636.

Fasshauer, D., Otto, H., Eliason, W. K., Jahn, R., and Brunger, A. T. (1997). Structural changes are associated with soluble N-ethylmaleimide-sensitive fusion protein attachment protein receptor complex formation. J. Biol. Chem. *272*, 28036–28041.

Fernandez-Chacon, R., Konigstorfer, A., Gerber, S. H., Garcia, J., Matos, M. F., Stevens, C. F., Brose, N., Rizo, J., Rosenmund, C., and Sudhof, T. C. (2001). Synaptotagmin I functions as a calcium regulator of release probability. Nature *410*, 41–49.

Fernandez-Chacon, R., Shin, O. H., Konigstorfer, A., Matos, M. F., Meyer, A. C., Garcia, J., Gerber, S. H., Rizo, J., Sudhof, T. C., and Rosenmund, C.

(2002). Structure/function analysis of Ca^{2+} binding to the C2A domain of synaptotagmin 1. J. Neurosci. *22*, 8438–8446.

Fernandez, I., Arac, D., Ubach, J., Gerber, S. H., Shin, O., Gao, Y., Anderson, R. G., Sudhof, T. C., and Rizo, J. (2001). Three-dimensional structure of the synaptotagmin 1 C2B-domain: synaptotagmin 1 as a phospholipid binding machine. Neuron *32*, 1057–1069.

Frazier, A. A., Roller, C. R., Havelka, J. J., Hinderliter, A., and Cafiso, D. S. (2003). Membrane-bound orientation and position of the synaptotagmin I C2A domain by site-directed spin labeling. Biochemistry *42*, 96–105.

Geppert, M., Goda, Y., Hammer, R. E., Li, C., Rosahl, T. W., Stevens, C. F., and Sudhof, T. C. (1994). Synaptotagmin I: a major Ca^{2+} sensor for transmitter release at a central synapse. Cell *79*, 717–727.

Gerona, R. R., Larsen, E. C., Kowalchyk, J. A., and Martin, T. F. (2000). The C terminus of SNAP25 is essential for Ca^{2+}-dependent binding of synaptotagmin to SNARE complexes. J. Biol. Chem. *275*, 6328–6336.

Giraudo, C. G., Eng, W. S., Melia, T. J., and Rothman, J. E. (2006). A clamping mechanism involved in SNARE-dependent exocytosis. Science *313*, 676–680.

Hayashi, T., McMahon, H., Yamasaki, S., Binz, T., Hata, Y., Sudhof, T. C., and Niemann, H. (1994). Synaptic vesicle membrane fusion complex: action of clostridial neurotoxins on assembly. EMBO J. *13*, 5051–5061.

Katz, B., and Miledi, R. (1965). The effect of calcium on acetylcholine release from motor nerve terminals. Proc. R. Soc. Lond. B Biol. Sci. *161*, 496–503.

Kee, Y., and Scheller, R. H. (1996). Localization of synaptotagmin-binding domains on syntaxin. J. Neurosci. *16*, 1975–1981.

Li, C., Ullrich, B., Zhang, J. Z., Anderson, R. G., Brose, N., and Sudhof, T. C. (1995). Ca^{2+}-dependent and -independent activities of neural and non-neural synaptotagmins. Nature *375*, 594–599.

Littleton, J. T., Bai, J., Vyas, B., Desai, R., Baltus, A. E., Garment, M. B., Carlson, S. D., Ganetzky, B., and Chapman, E. R. (2001). Synaptotagmin mutants reveal essential functions for the C2B domain in Ca^{2+}-triggered fusion and recycling of synaptic vesicles in vivo. J. Neurosci. *21*, 1421–1433.

Littleton, J. T., Stern, M., Perin, M., and Bellen, H. J. (1994). Calcium dependence of neurotransmitter release and rate of spontaneous vesicle fusions are altered in *Drosophila* synaptotagmin mutants. Proc. Natl. Acad. Sci. USA *91*, 10888–10892.

Littleton, J. T., Stern, M., Schulze, K., Perin, M., and Bellen, H. J. (1993). Mutational analysis of *Drosophila* synaptotagmin demonstrates its essential role in Ca^{2+}-activated neurotransmitter release. Cell *74*, 1125–1134.

Lynch, K. L., and Martin, T. F. (2007). Synaptotagmins I and IX function redundantly in regulated exocytosis but not endocytosis in PC12 cells. J. Cell Sci.

Marcia, R. F., Mitchell, J. C., and Rosen, J. B. (2005). Iterative convex quadratic approximation for global optimization in protein docking. Comp. Opt. Appl. *32*, 285–297.

Murray, D., and Honig, B. (2002). Electrostatic control of the membrane targeting of C2 domains. Mol. Cell *9*, 145–154.

Nonet, M. L., Grundahl, K., Meyer, B. J., and Rand, J. B. (1993). Synaptic function is impaired but not eliminated in *C. elegans* mutants lacking synaptotagmin. Cell *73*, 1291–1305.

Paddison, P. J., Caudy, A. A., Bernstein, E., Hannon, G. J., and Conklin, D. S. (2002). Short hairpin RNAs (shRNAs) induce sequence-specific silencing in mammalian cells. Genes Dev. *16*, 948–958.

Pang, Z. P., Shin, O. H., Meyer, A. C., Rosenmund, C., and Sudhof, T. C. (2006). A gain-of-function mutation in synaptotagmin-1 reveals a critical role of Ca^{2+}-dependent soluble N-ethylmaleimide-sensitive factor attachment protein receptor complex binding in synaptic exocytosis. J. Neurosci. *26*, 12556–12565.

Poirier, M. A., Xiao, W., Macosko, J. C., Chan, C., Shin, Y. K., and Bennett, M. K. (1998). The synaptic SNARE complex is a parallel four-stranded helical bundle. Nat. Struct. Biol. *5*, 765–769.

Reim, K., Mansour, M., Varoqueaux, F., McMahon, H. T., Sudhof, T. C., Brose, N., and Rosenmund, C. (2001). Complexins regulate a late step in Ca^{2+}-dependent neurotransmitter release. Cell *104*, 71–81.

Rhee, J. S., Li, L. Y., Shin, O. H., Rah, J. C., Rizo, J., Sudhof, T. C., and Rosenmund, C. (2005). Augmenting neurotransmitter release by enhancing the apparent Ca^{2+} affinity of synaptotagmin 1. Proc. Natl. Acad. Sci. USA *102*, 18664–18669.

Rizo, J., Chen, X., and Arac, D. (2006). Unraveling the mechanisms of synaptotagmin and SNARE function in neurotransmitter release. Trends Cell Biol. *16*, 339–350.

Rizo, J., and Sudhof, T. C. (1998). Mechanics of membrane fusion. Nat. Struct. Biol. *5*, 839–842.

Schaub, J. R., Lu, X., Doneske, B., Shin, Y. K., and McNew, J. A. (2006). Hemifusion arrest by complexin is relieved by Ca^{2+}-synaptotagmin I. Nat. Struct. Mol. Biol. *13*, 748–750.

Schiavo, G., Stenbeck, G., Rothman, J. E., and Sollner, T. H. (1997). Binding of the synaptic vesicle v-SNARE, synaptotagmin, to the plasma membrane t-SNARE, SNAP-25, can explain docked vesicles at neurotoxin-treated synapses. Proc. Natl. Acad. Sci. USA *94*, 997–1001.

Shao, X., Davletov, B. A., Sutton, R. B., Sudhof, T. C., and Rizo, J. (1996). Bipartite Ca^{2+}-binding motif in C2 domains of synaptotagmin and protein kinase C. Science *273*, 248–251.

Shao, X., Fernandez, I., Sudhof, T. C., and Rizo, J. (1998). Solution structures of the Ca^{2+}-free and Ca^{2+}-bound C2A domain of synaptotagmin I: does Ca^{2+} induce a conformational change? Biochemistry *37*, 16106–16115.

Shao, X., Li, C., Fernandez, I., Zhang, X., Sudhof, T. C., and Rizo, J. (1997). Synaptotagmin-syntaxin interaction: the C2 domain as a Ca^{2+}-dependent electrostatic switch. Neuron *18*, 133–142.

Sollner, T., Bennett, M. K., Whiteheart, S. W., Scheller, R. H., and Rothman, J. E. (1993a). A protein assembly-disassembly pathway in vitro that may correspond to sequential steps of synaptic vesicle docking, activation, and fusion. Cell *75*, 409–418.

Sollner, T., Whiteheart, S. W., Brunner, M., Erdjument-Bromage, H., Geromanos, S., Tempst, P., and Rothman, J. E. (1993b). SNAP receptors implicated in vesicle targeting and fusion. Nature *362*, 318–324.

Stevens, C. F., and Sullivan, J. M. (2003). The synaptotagmin C2A domain is part of the calcium sensor controlling fast synaptic transmission. Neuron *39*, 299–308.

Sudhof, T. C. (2002). Synaptotagmins: why so many? J. Biol. Chem. *277*, 7629–7632.

Sutton, R. B., Davletov, B. A., Berghuis, A. M., Sudhof, T. C., and Sprang, S. R. (1995). Structure of the first C2 domain of synaptotagmin I: a novel Ca^{2+}/phospholipid-binding fold. Cell *80*, 929–938.

Sutton, R. B., Ernst, J. A., and Brunger, A. T. (1999). Crystal structure of the cytosolic C2A-C2B domains of synaptotagmin III. Implications for Ca^{2+}-independent snare complex interaction. J. Cell Biol. *147*, 589–598.

Sutton, R. B., Fasshauer, D., Jahn, R., and Brunger, A. T. (1998). Crystal structure of a SNARE complex involved in synaptic exocytosis at 2.4 A resolution. Nature *395*, 347–353.

Tang, J., Maximov, A., Shin, O. H., Dai, H., Rizo, J., and Sudhof, T. C. (2006). A complexin/synaptotagmin 1 switch controls fast synaptic vesicle exocytosis. Cell *126*, 1175–1187.

Tokumaru, H., Umayahara, K., Pellegrini, L. L., Ishizuka, T., Saisu, H., Betz, H., Augustine, G. J., and Abe, T. (2001). SNARE complex oligomerization by synaphin/complexin is essential for synaptic vesicle exocytosis. Cell *104*, 421–432.

Tucker, W. C., Edwardson, J. M., Bai, J., Kim, H. J., Martin, T. F., and Chapman, E. R. (2003). Identification of synaptotagmin effectors via acute inhibition of secretion from cracked PC12 cells. J. Cell Biol. *162*, 199–209.

Tucker, W. C., Weber, T., and Chapman, E. R. (2004). Reconstitution of Ca^{2+}-regulated membrane fusion by synaptotagmin and SNAREs. Science *304*, 435–438.

Ubach, J., Zhang, X., Shao, X., Sudhof, T. C., and Rizo, J. (1998). Ca^{2+} binding to synaptotagmin: how many Ca^{2+} ions bind to the tip of a C2-domain? EMBO J. *17*, 3921–3930.

Wang, P., Wang, C. T., Bai, J., Jackson, M. B., and Chapman, E. R. (2003). Mutations in the effector binding loops in the C2A and C2B domains of synaptotagmin I disrupt exocytosis in a nonadditive manner. J. Biol. Chem. *278*, 47030–47037.

Weber, T., Zemelman, B. V., McNew, J. A., Westermann, B., Gmachl, M., Parlati, F., Sollner, T. H., and Rothman, J. E. (1998). SNAREpins: minimal machinery for membrane fusion. Cell *92*, 759–772.

Yoshihara, M., Adolfsen, B., and Littleton, J. T. (2003). Is synaptotagmin the calcium sensor? Curr. Opin. Neurobiol. *13*, 315–323.

Zhang, X., Kim-Miller, M. J., Fukuda, M., Kowalchyk, J. A., and Martin, T. F. (2002). Ca^{2+}-dependent synaptotagmin binding to SNAP-25 is essential for Ca^{2+}-triggered exocytosis. Neuron *34*, 599–611.

Zhang, X., Rizo, J., and Sudhof, T. C. (1998). Mechanism of phospholipid binding by the C2A-domain of synaptotagmin I. Biochemistry *37*, 12395–12403.